Thermodynamics of Tryptophan-Mediated Activation of the *trp* RNA-Binding Attenuation Protein†

Craig A. McElroy,‡ Amanda Manfredo,§ Paul Gollnick,§ and Mark P. Foster*,‡,||

Ohio State Biochemistry Program and Biophysics Program and Protein Research Group, Department of Biochemistry, The Ohio State University, Columbus, Ohio 43210, and Department of Biological Sciences, State University of New York, Buffalo, New York 14260

Received December 21, 2005; Revised Manuscript Received March 15, 2006

ABSTRACT: The *trp R*NA-binding *a*ttenuation *p*rotein (TRAP) functions in many bacilli to control the expression of the tryptophan biosynthesis genes. Transcription of the *trp* operon is controlled by TRAP through an attenuation mechanism, in which competition between two alternative secondary-structural elements in the 5′ leader sequence of the nascent mRNA is influenced by tryptophan-dependent binding of TRAP to the RNA. Previously, NMR studies of the undecamer (11-mer) suggested that tryptophan-dependent control of RNA binding by TRAP is accomplished through ligand-induced changes in protein dynamics. We now present further insights into this ligand-coupled event from hydrogen/deuterium (H/D) exchange analysis, differential scanning calorimetry (DSC), and isothermal titration calorimetry (ITC). Scanning calorimetry showed tryptophan dissociation to be independent of global protein unfolding, while analysis of the temperature dependence of the binding enthalpy by ITC revealed a negative heat capacity change larger than expected from surface burial, a hallmark of binding-coupled processes. Analysis of this excess heat capacity change using parameters derived from protein folding studies corresponds to the ordering of 17−24 residues per monomer of TRAP upon tryptophan binding. This result is in agreement with qualitative analysis of residue-specific broadening observed in TROSY NMR spectra of the 91 kDa oligomer. Implications for the mechanism of ligand-mediated TRAP activation through a shift in a preexisting conformational equilibrium and an induced-fit conformational change are discussed.

The undecameric (11-mer) *trp* RNA-binding attenuation protein (TRAP) controls the transcription (*1*−*5*), and in some cases the translation (*6*−*11*), of the genes responsible for tryptophan biosynthesis in many bacilli. Transcriptional regulation of the *trp* operon in these bacilli is achieved through attenuation, in which competing secondary-structural elements in the 5′ leader region of the nascent mRNA control the extent of transcriptional read-through of the structural genes (*3*−*5*). TRAP exercises transcriptional control by influencing the formation of these secondary-structural elements through tryptophan-dependent binding to the RNA. When tryptophan is limiting, TRAP is inactive and does not bind to the RNA. This allows a stable antiterminator hairpin to form, promoting transcriptional read-through of the entire operon. However, when the intracellular tryptophan level is sufficiently high, TRAP binds to tryptophan and becomes activated to bind to 11 triplet repeats of (G/U)AG's present in the 5′ leader region of the mRNA. When TRAP is bound, the antiterminator RNA structure cannot form, allowing preferential formation of the terminator hairpin, thereby halting transcription (*3*−*5*).

The crystal structures of tryptophan-activated *Bacillus stearothermophilus* TRAP in binary complex with tryptophan (1QAW) (*12*) and in ternary complex with tryptophan and RNA (1C9S) (*13*, *14*) reveal an oligomer of 11 identical subunits related by an 11-fold rotational axis of symmetry. The structure is comprised of 11 antiparallel β-sheets, with each sheet consisting of three strands from one subunit and four strands from the neighboring subunit (Figure 1). The tryptophan ligand is completely buried between the β-sheets at the interface between subunits in a cavity that is largely apolar with a few polar side-chain and backbone moieties making hydrogen bond contacts to the side chain amide and backbone amino and carboxyl groups of the tryptophan (*12*, *14*−*16*). The bound RNA wraps around the protein with conserved bases making specific contacts with TRAP residues (*13*, *16*−*19*).

Until recently, limited data were available on the structure of inactivate apo-TRAP; therefore, little was known about the allosteric mechanism of tryptophan activation of TRAP for RNA binding. The oligomeric state of TRAP (11-mer) is not altered by tryptophan, remaining oligomeric over a wide range of concentrations (10^{-6}−10^{-2} M), ruling out assembly as an activation mechanism (*20*−*22*). TROSY NMR studies of the 91 kDa TRAP protein both free and bound to tryptophan revealed severe exchange broadening

† This work was supported by a structural biology supplement from the National Institutes of Health (Award Number GM62750-01 to P.G.) and is based upon work supported by the National Science Foundation under Award Number MCB-0092962 to M.P.F. C.A.M. was supported in part by NIH Training Grant T32GM008512.

* Corresponding author. Phone: 614-292-1377. Fax: 614-292-6773. E-mail: foster.281@osu.edu.

‡ Ohio State Biochemistry Program, The Ohio State University.

§ Department of Biological Sciences, State University of New York.

|| Biophysics Program and Protein Research Group, Department of Biochemistry, The Ohio State University.

10.1021/bi0526074 CCC: $33.50
Published on Web 06/01/2006

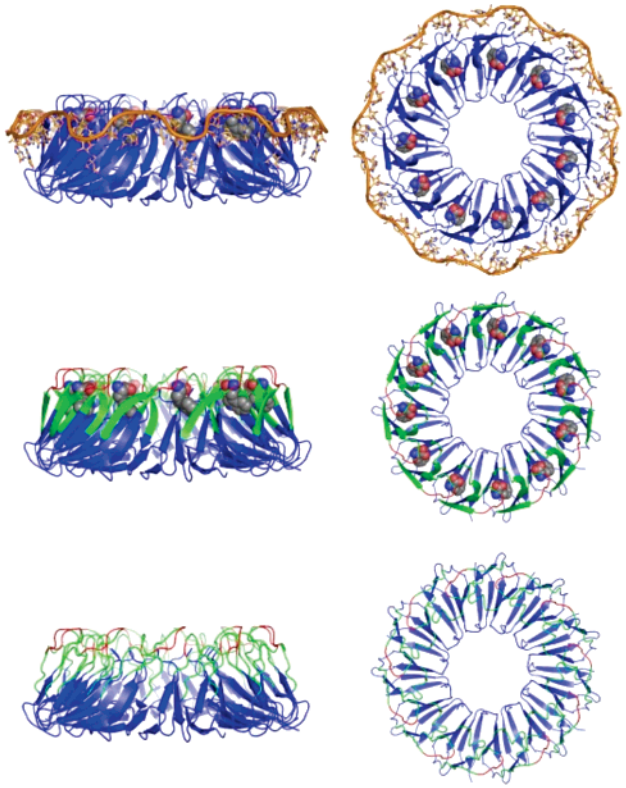

FIGURE 1: Structures and model of TRAP activation (left/right, side/top views). Crystal structures of *B. stearothermophilus* TRAP in ternary complex with tryptophan and RNA [top; 1C9S (*13*)] and in binary complex with tryptophan [middle; 1QAW (*14*)]. (Top) The 11 subunits are displayed as blue cartoons, the tryptophan ligands are shown in CPK, and the RNA is in orange. The tryptophan ligands are buried in the interface between subunits, and the RNA wraps around the perimeter of the TRAP oligomer making contacts to β-sheet residues. (Bottom) Model of the structure of TRAP in the absence of tryptophan illustrating dynamic disorder of residues in the Trp- and RNA-binding regions of the protein (*21*). (Middle, bottom) Loop residues that exhibited severe exchange broadening in NMR spectra of apo-TRAP are in green, while loop residues in red were exchange-broadened in both apo- and holo-TRAP; in addition, residues 1−8 and 71−74 could not be assigned for either state (*21*).

for the backbone amide resonances of 19 residues in the tryptophan- and RNA-binding regions of the protein (see Figures 1 and 2), while limited proteolysis revealed a ligand-dependent change in proteolytic accessibility for this region (*21*). Analytical ultracentrifugation studies of apo- and holo-TRAP (*22*) also suggest that holo-TRAP is more tightly packed than apo-TRAP, consistent with the protein becoming more structured upon tryptophan binding. These findings are consistent with the proposal that tryptophan activates TRAP to bind to its RNA target through binding-coupled folding of the RNA-binding surface of TRAP (*21*).

Here we report results aimed at providing a thermodynamic description of the tryptophan binding-coupled transition that leads to TRAP activation. Hydrogen/deuterium (H/D) exchange experiments revealed increased protection of amide resonances upon binding tryptophan. A binding titration monitored by intrinsic tryptophan fluorescence indicated that the 11 tryptophan ligands bind to TRAP noncooperatively. Scanning calorimetry showed that ligand dissociation involves a large thermal event separate from global protein unfolding. The binding-associated heat capacity change (ΔC_p) measured by isothermal titration calorimetry

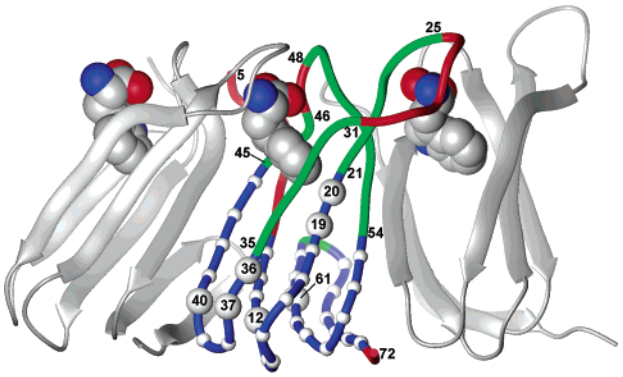

FIGURE 2: Close-up view of tryptophan-mediated spectral perturbations. Two adjacent subunits in the undecamer are shown in gray, and tryptophan ligands are drawn as CPK. For the middle protomer the same color scheme is used as in Figure 1. Small spheres identify residues whose backbone amide hydrogens exhibited no measurable exchange with deuterium (H/D exchange) in either apo- or holo-TRAP, while the large spheres identify residues whose H/D exchange rate was reduced upon tryptophan binding (see Figure 4).

(ITC) revealed a larger ΔC_p than expected from burial of solvent-accessible surface area (*23*−*30*). Interpretation of the excess ΔC_p using protein folding models yields qualitative agreement with residue-specific conformational exchange broadening of residues in apo-TRAP. These results are consistent with a model in which TRAP activation proceeds through a mechanism involving both selection from a preexisting conformational equilibrium and an induced-fit conformational change.

MATERIALS AND METHODS

Preparation of Apo-TRAP. B. stearothermophilus TRAP was expressed in *Escherichia coli* and purified as described previously (*21*). Although tryptophan binding is relatively weak (~1 μM), complete removal of the tryptophan from TRAP by dialysis is inefficient. Therefore, to remove the tryptophan that copurifies with the protein, TRAP was purified by reversed-phase HPLC on a 1 × 25 cm C4 column (Vydac model 214TP) at a flow rate of 3 mL/min using a gradient elution with 0.1% (v/v) trifluoroacetic acid (TFA) (Sigma) in water (buffer A) and 0.1% TFA in acetonitrile (buffer B). The gradient elution consisted of a 15 mL wash with 5% buffer B, a 30 mL gradient from 5% to 20% buffer B, a 30 mL wash with 20% buffer B (during which the tryptophan eluted), and a 90 mL gradient from 20% to 70% buffer B, where TRAP eluted between 40% and 60% acetonitrile. The fractions containing TRAP were then lyophilized, and the powder (~32 mg) was dissolved in 3 mL of 6 M guanidine hydrochloride (GdnHCl), 50 mM sodium phosphate at pH 8.0, and 100 mM sodium chloride (NaCl). The resuspended TRAP was placed in a 3500 Da cutoff dialysis cassette (Pierce) and dialyzed against 0.5 L of 3 M GdnHCl, 50 mM sodium phosphate at pH 8.0, and 100 mM NaCl for 12 h at 55 °C. The GdnHCl was then diluted to 1.5 M with 50 mM sodium phosphate at pH 8.0 and 100 mM NaCl (buffer C), and the protein was dialyzed for an additional 12 h at 55 °C. The protein was then dialyzed against 4 L of buffer C for 24 h at 55 °C, followed by an additional dialysis against 4 L of buffer C for 48 h at 4 °C. Previous studies have shown that TRAP can be denatured into unfolded monomers by GdnHCl and then renatured into

Table 1: Temperature-Dependent Thermodynamics for the Titration of Tryptophan into TRAP[a]

temp	*n*	ΔG	ΔH	$T\Delta S$	K_A (/10^6)
298	10.97 ± 0.03	−9.55 ± 0.06	−13.88 ± 0.09	−4.33 ± 0.11	9.75 ± 0.16
303	11.07 ± 0.09	−9.43 ± 0.01	−15.60 ± 0.06	−6.17 ± 0.07	6.28 ± 0.24
308	10.77 ± 0.29	−9.35 ± 0.01	−17.37 ± 0.07	−8.02 ± 0.07	4.24 ± 0.05
313	10.40 ± 0.10	−9.22 ± 0.32	−19.13 ± 0.25	−9.91 ± 0.41	2.72 ± 0.16
318	10.16 ± 0.23	−9.13 ± 0.01	−21.10 ± 0.43	−11.97 ± 0.43	1.83 ± 0.04
323	10.53 ± 0.24	−8.98 ± 0.02	−23.03 ± 0.04	−14.05 ± 0.05	1.17 ± 0.05

[a] Reported errors are the standard deviation of three repeat data sets at each temperature. Values of ΔH, TΔS, and ΔG are in kcal mol^{-1}, T is in kelvin, K_A is in M^{-1}, and n is the number of tryptophan binding sites per TRAP oligomer.

fully functional 11-mers by simply removing the denaturant (*20*). The efficacy of the refolding procedure was confirmed by the ITC experiments, which yielded an *n*-value close to 11 (10.16−11.07, Table 1) for each oligomer. Distilled, deionized water (MilliQ; Millipore, Inc.) was used for all buffers.

H/D Exchange of TRAP. Apo- and holo-TRAP were exchanged into 90/10 ($^2H_2O/^1H_2O$) by a 10-fold dilution into buffer C in 99.9% ^2H_2O, adjusting the pH to account for the pH/pD difference (*31*). TRAP was then concentrated using an ultrafiltration centrifugal concentrator (Amicon). The first time point was taken approximately 1 h after exchanging into ^2H_2O. Two-dimensional $^1H-^{15}N$ TROSY NMR spectra (*32*) were recorded on an 800 MHz NMR spectrometer at 55 °C, every hour for the first 24 h, with additional time points taken after 48 h and 1 week; samples were stored at 55 °C between spectra.

Tryptophan Fluorescence. Protein concentration was estimated using the native extinction coefficient, 2798.6 M^{-1} cm^{-1} at 276 nm, determined using the theoretical extinction coefficient, 2900 M^{-1} cm^{-1} at 276 nm, and comparing the absorbance under denaturing (6 M GdnHCl and 100 mM sodium phosphate at pH 6.5) and native conditions (50 mM sodium phosphate at pH 8.0, 100 mM NaCl) (*33*). The tryptophan concentration was determined using the extinction coefficient 5579 M^{-1} cm^{-1}at 278 nm (*34*). For the concentrated solutions of protein or tryptophan, errors in the estimation of the concentrations were obtained from two different dilutions; for the dilute solutions, errors are the deviation of two measurements taken on the same solution. To ensure that the buffer conditions of the protein and ligand were identical, tryptophan (Sigma) was dissolved in the dialysate from the last dialysis of TRAP. All fluorescence experiments were performed on a Fluoromax-3 fluorometer with an excitation wavelength of 295 nm, an integration time of 0.1 s, five scan signal averaging, a slit width of 2 nm, and scans taken from 300 to 450 nm at 1 nm increments. The cell contained 2.8 ± 0.2 μM tryptophan and was titrated with 46.3 ± 0.3 μM apo-TRAP oligomer. Binding was monitored from the emission intensity at 332 nm after each addition of TRAP, and the fraction of bound tryptophan was calculated from

$$r_i = (I_i - I_f)/(I_b - I_f) \quad (1)$$

where r_i is the fraction of bound tryptophan after the ith addition of TRAP, I_i is the signal intensity at 332 nm after the ith addition of TRAP, I_f is the intensity at 332 nm of free tryptophan, and I_b is the intensity at 332 nm of fully bound tryptophan. The resultant data were fit to a standard binding quadratic:

$$r_i = 1 - \{([W]_T + [T]_T n + K_d) - \sqrt{([W]_T + [T]_T n + K_d)^2 - 4n[W]_T[T]_T}\}/2[W]_T \quad (2)$$

where r_i is the fraction of bound tryptophan, n is the number of binding sites, K_d is the dissociation constant, $[W]_T$ is the total tryptophan concentration, and $[T]_T$ is the total TRAP oligomer concentration. The Hill coefficient was determined by taking the slope of the best fit line from the plot of log($r_i/(1 - r_i)$) versus log $[T]_f$ (the free TRAP concentration).

ITC of TRAP. Protein and tryptophan concentrations were estimated as described above. All ITC data were obtained on a MicroCal VP-ITC with a 3 μL first injection followed by 5 μL injections with a spacing of 220 s between injections. The cell contained TRAP at a concentration of 5.1 ± 0.6 μM oligomer, and the syringe contained 662.1 ± 12.0 μM tryptophan. The exothermic heat pulse detected after each injection was integrated, the heat of dilution subtracted from the integrated value, and the corrected heat value divided by the total moles of tryptophan injected. The resulting values were plotted as a function of the molar ratio of TRAP oligomer and fit to a one binding site model using a nonlinear least-squares method (Figure 5; Origin v.7, MicroCal); ΔS values were obtained via Gibbs' relation from the fitted K_A and ΔH values. All experiments were performed in triplicate; reported errors are the standard deviation in the fitted values between the three data sets. Although the extremely low extinction coefficient of TRAP leads to ~10% uncertainty in the protein concentration, the samples used for the ITC studies were prepared simultaneously from the same stock solution. Consequently, the small variation in the measured parameters reflects the exceptional signal-to-noise ratio of the titration data, not the uncertainty in the protein concentration. To subtract the heat of dilution for both ligand and protein simultaneously, baseline runs were performed using the fully titrated TRAP (after removing the excess volume and refilling the syringe with ligand). The heat capacity change was obtained from a linear fit of the enthalpy data to

$$\Delta H(T) = \Delta C_p(T - T_h) \quad (3)$$

where T_h is the temperature at which the binding enthalpy is zero. The temperature at which the entropic contribution to binding is zero (T_s) was obtained from fitting the temperature dependence of the binding free energy to the modified Gibbs−Helmholtz equation:

$$\Delta G(T) = -RT \ln K_a = \Delta C_p(T - T_h) - T\Delta C_p \ln(T/T_s) \quad (4)$$

Differential Scanning Calorimetry. Protein and tryptophan concentrations were estimated as described above. All DSC data were acquired on a MicroCal VP-DSC with a scan rate of 60 °C/h, scans were taken from 25 to 130 °C at a starting pressure of 29 psi, and cells were refilled at 27 °C. The protein concentration for apo-TRAP was 51.1 μM TRAP (562.3 μM monomer) and for holo-TRAP was 50.0 μM (550.5 μM monomer). Tryptophan (26.6 mM) was added to a final concentration of 560 μM in the holo-TRAP sample. Data were normalized to the protein concentration, and the holo-TRAP data were *y*-axis translated to make the initial baselines for the apo- and holo-TRAP data coincident using Origin v.7 (MicroCal).

Solvent-Accessible Surface Area and ΔC_p^{calc}. Solvent-accessible surface areas (ASA) of both the tryptophan ligand and the tryptophan-binding cavities of TRAP were determined using STC v. 5.0 (*35*) with extended atom radii and a probe radius of 1.4 Å. To measure the change in solvent-accessible surface area upon tryptophan binding, separate PDB files were constructed containing one protomer of TRAP and one tryptophan ligand from the crystal structure of the binary complex of tryptophan with *B. stearothermophilus* TRAP (1QAW) (*14*). In all, 23 files were generated, two for each protomer (one with each of the two tryptophan ligands that are contacted by that protomer). The average polar and nonpolar solvent-accessible surface areas of the tryptophan ligands were obtained from the STC calculated values for the free tryptophans. The average change in polar and nonpolar solvent-accessible surface area of the tryptophan-binding pockets was calculated by adding the change in solvent-accessible surface area for the two protomers that contact the same tryptophan. The overall change in polar and nonpolar solvent-accessible surface is the sum of the solvent-accessible surface area of the tryptophan and the solvent-accessible surface area of the binding pocket. The heat capacity change expected from the structural data (ΔC_p^{calc}) was calculated from the change in ASA using (*28*)

$$\Delta C_p^{calc} = 0.32(\Delta A_{np}) - 0.14(\Delta A_p) \quad (5)$$

where ΔA_p is the change in polar solvent-accessible surface area, ΔA_{np} is the change in nonpolar solvent-accessible surface area.

Proton and Ion Linkage Effects. To determine whether proton or ion linkage contributes to the heat capacity of tryptophan binding to TRAP (*30*, *36*−*38*), apo-TRAP was prepared as described above, but with one additional dialysis step. After refolding, the resultant protein was split into seven aliquots, which were placed into separate 3500 Da cutoff dialysis cassettes and dialyzed into the appropriate buffers. Buffers used to test for ion linkage (*38*) were 50 mM sodium phosphate at pH 8.0 with no NaCl, 100 mM NaCl, 250 mM NaCl, and 500 mM NaCl. The buffers used for analysis of proton-linkage contributions were 50 mM sodium phosphate at pH 8.0 and 100 mM NaCl, 20 mM Tris at pH 8.0 and 100 mM NaCl, and 20 mM HEPES at pH 8.0 and 100 mM NaCl; ionization enthalpies used were as reported (*37*).

ΔC_p *and Binding-Coupled Folding.* As proposed by Spolar and Record (*28*), the experimentally measured heat capacity change was used to estimate the loss in protein conformational entropy upon binding tryptophan. Once the contributions to ΔC_p from other sources were determined (*30*, *36*−*38*), the remaining (excess) heat capacity was used to calculate the contribution to association from the hydrophobic effect (ΔS_{HE}):

$$\Delta S_{HE} = 1.35\Delta C_p \ln(T/386) \quad (7)$$

where the factor 1.35 assumes a $\Delta A_p/\Delta A_{np} = 0.59$ (which is approximately the case in the folding of globular proteins) (*28*), and 386 K is the temperature at which the entropy contribution of the hydrophobic effect vanishes (*23*). The entropy of association (ΔS_{assoc}) can be further dissected at the characteristic temperature (T_s) where the overall association entropy change is zero:

$$\Delta S_{assoc}(T_s) = \Delta S_{HE} + \Delta S_{rt} + \Delta S_{other} = 0 \quad (8)$$

where ΔS_{rt} is the change in entropy due to loss of rotational and translational freedom and ΔS_{other} is the change in entropy due to other events attributed predominantly to the loss of conformational mobility upon protein folding (*28*). Since at the T_s the change in entropy of molecular association is zero, the magnitude of ΔS_{HE} must equal the sum of ΔS_{rt} and ΔS_{other}. For molecular associations in which no conformational rearrangements of the ligand or receptor occur (rigid-body association), ΔS_{other} should be negligible and ΔS_{HE} should be entirely balanced by ΔS_{rt}. Analysis of a number of proteins for which structural information suggests that there are no binding-coupled conformational rearrangements or folding yields an empirical estimate for ΔS_{rt} of -50 ± 10 cal K^{-1} mol^{-1} (*28*). Thus, from the remainder (ΔS_{other}) one obtains an estimate of the change in protein conformation entropy upon ligand binding.

Empirical studies of the thermodynamics of protein folding suggest that the unfavorable entropic cost of protein folding is relatively constant when expressed per residue, $\Delta S_{\mathscr{R}}$, although reported values are somewhat dependent on the data set used to derive it (*28*, *39*, *40*), ranging from -4.1 to -5.6 cal K^{-1} (mol of residue)$^{-1}$. This value can be used to estimate the number of residues that become folded upon binding ($\mathscr{R}$) from

$$\mathscr{R} = \frac{\Delta S_{other}}{\Delta S_{\mathscr{R}}} = \frac{1.35\Delta C_p \ln(T_s/386) - \Delta S_{rt}}{\Delta S_{\mathscr{R}}} \quad (9)$$

Estimation of ΔC_p *for Binding-Coupled Folding from Structural Data.* The 19 residues in the tryptophan- and RNA-binding sites that become exchange-broadened upon removal of ligand (21−25, 31−35, 45−46, and 48−54), were modeled in an extended conformation using MOLMOL (*41*), and ASA calculations were performed using STC v.5.0 (*35*) with both the extended structures and the tryptophan treated as the "ligand" for the calculations. Although the use of fully extended conformations for these loops will result in an overestimate of the ASA change upon folding of these residues, in the absence of accurate models of the loops in apo-TRAP, use of the extended conformation provides an upper limit for the ASA change. The ASA buried by the linkage between the structured and unstructured regions was subtracted from the total ASA, and the resulting value was used to calculate the ΔC_p for binding-coupled folding using eq 5. Inclusion of the six loop residues that remain exchange-broadened in Trp-bound TRAP (26−30 and 47, shown in

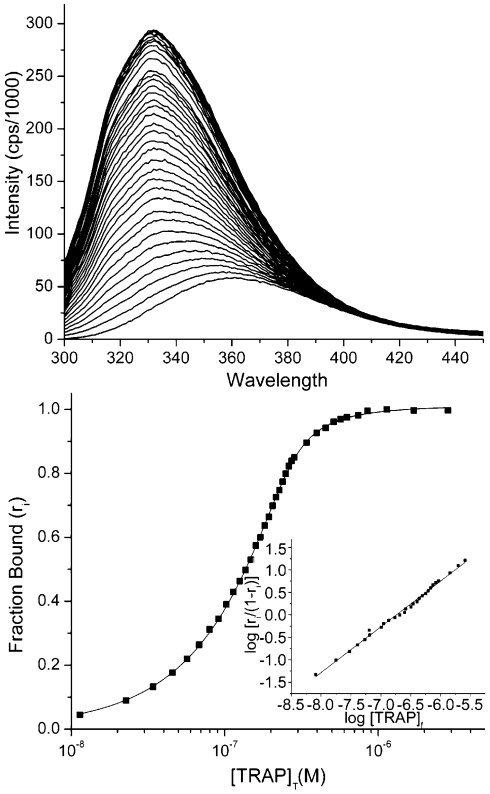

FIGURE 3: Noncooperative binding of tryptophan to TRAP. (Top) Titration of tryptophan with TRAP monitored by tryptophan fluorescence (25 °C). (Bottom) A typical binding isotherm for TRAP binding tryptophan (squares) with a nonlinear fit to eq 2 (line); at 25 °C the dissociation constant (K_d) was 0.16 ± 0.01 μM, with a best-fit stoichiometry of 10.6 ± 0.9 tryptophans per TRAP 11-mer. Inset: Hill plot demonstrating lack of cooperativity in tryptophan binding to TRAP; the Hill coefficient is 1.02 ± 0.01 (slope of the best-fit line).

red in Figure 2) would increase the estimated ASA change roughly proportionally (~30%).

RESULTS AND DISCUSSION

Tryptophan Binding to B. stearothermophilus TRAP Is Noncooperative. Prior to detailed analysis of the mechanism of TRAP activation, we examined whether tryptophan binding to *B. stearothermophilus* TRAP is cooperative. We monitored binding of TRAP to tryptophan at 25 °C using the change in intrinsic fluorescence of the latter upon binding (Figure 3). The wavelength for the emission maximum of tryptophan fluorescence shows the typical blue shift (from 357 to 332 nm) and increase in intensity (~6-fold) that is expected upon transfer of tryptophan from a polar to nonpolar environment (*42*). The data were well described by a single-site binding quadratic (Figure 3, bottom) and were fit with an equilibrium binding constant, K_A, of 6.32 ± 0.3 × 10^6 M^{-1}. Analysis of the binding data using a Hill plot (Figure 3, inset) yielded highly linear data with a Hill coefficient near unity. Titrations repeated over a range of temperatures (*25*−*70*) yielded similar Hill coefficients (not shown). Thus, although there are 11 tryptophan-binding sites in each TRAP oligomer, this analysis indicates that tryptophan binding to *B. stearothermophilus* TRAP can be reasonably treated as involving 11 identical and independent sites, instead of requiring the use of more complicated partition functions (*43*).

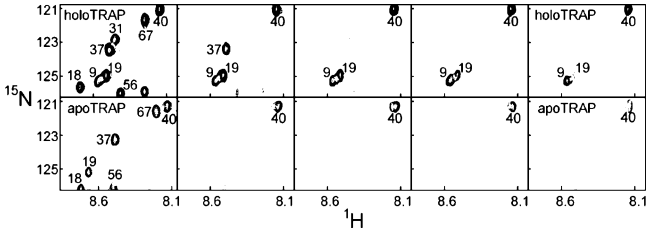

FIGURE 4: Hydrogen/deuterium exchange in apo- and holo-TRAP. An expanded region of ^{1}H−^{15}N correlation spectra of apo- (bottom) and holo- (top) TRAP recorded before and at a series of time intervals (left to right: 0, 1, 5, 9, and 15 h) after exchange into 90/10 $^2H_2O/^1H_2O$.

Structural Changes upon Tryptophan Binding: H/D Exchange. On the basis of site-specific NMR resonance line broadening we previously proposed that ligand binding to TRAP involved a ligand-mediated change in protein dynamics: coupled folding (*21*). The structure of holo-TRAP reveals an all-β-sheet protein (*12*, *14*); therefore, if tryptophan binding leads to stabilization of secondary-structural elements, one might expect a concomitant increase in β-sheet signature in the circular dichroism (CD) spectrum. However, the relative inaccuracy of quantitating β-sheet structure (*44*, *45*), coupled with interference from the tryptophan ligand (*46*, *47*), rendered CD studies uninformative of ligand-induced structural changes (data not shown). On the other hand, ligand-induced stabilization of the protein structure could be ascertained from hydrogen/deuterium (H/D) exchange experiments.

If folding were coupled to ligand binding, upon tryptophan addition to TRAP the amide hydrogens of residues involved in the folding transition should show increased protection from exchange with solvent. Unfortunately, the majority of the TRAP residues of most interest (i.e., those in the tryptophan- and RNA-binding regions, colored red and green in Figures 1 and 2) are broadened beyond detection in the apoprotein (*21*), preventing NMR-based measurement of the H/D exchange rates of these residues. Nevertheless, H/D exchange experiments (Figure 4) provided important insight into the ligand-induced structural changes in TRAP. Many of the amides show no measurable exchange even after 1 week, revealing the presence of an extremely stable structured core in both apo- and holo-TRAP. Thus, we conclude that the amides with measurable rates exchange via local, not global fluctuations in the protein structure. Increased protection from exchange in holo-TRAP is evident for several residues, including Ala12, Val19, Ile20, Leu36, Asp37, Glu40, and Ile61 (large spheres in Figure 2), reflecting local ligand-induced stabilization of the protein structure. The increased protection of amides from Asp37 and Glu40 (Figures 2 and 4) is particularly telling, since these residues are involved in RNA base recognition (*13*), reflecting the mechanism by which ligand binding is transmitted to the RNA-binding residues. These data are consistent with the hypothesis (*21*) that apo-TRAP is unable to bind RNA due to conformational disorder of the RNA-binding residues and that tryptophan binding likely proceeds through preferential binding to one conformation of a preexisting conformational equilibrium (*48*, *72*).

Thermodynamics of Tryptophan Binding to TRAP. Difficulties in characterizing the ligand-induced structural/dynamic changes in TRAP using spectroscopic techniques led us to use isothermal titration calorimetry (ITC) to measure

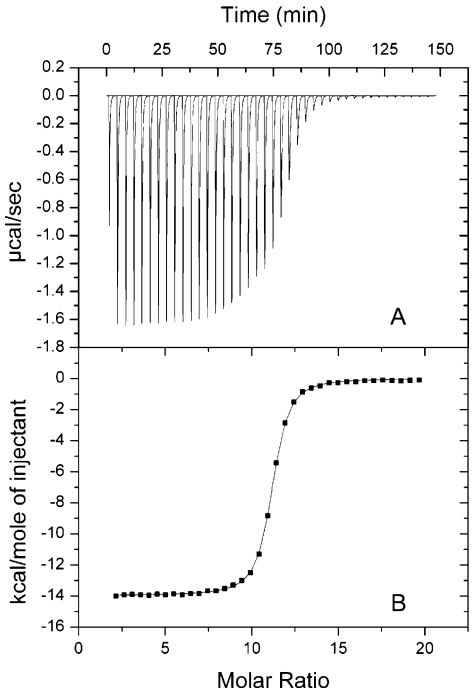

FIGURE 5: ITC of TRAP. (A) Thermogram from a titration of tryptophan into TRAP (25 °C) showing the change in power required to maintain a constant temperature difference between the sample and reference cells upon injections of tryptophan. (B) Time-integrated heat data normalized per mole of injectant (squares) with a nonlinear fit to the identical and independent sites model (line). Best-fit parameters are shown in Table 1.

the change in thermodynamic heat capacity (ΔC_p) as a means of characterizing binding-coupled changes in protein structure (*23*−*28*, *30*). Excellent quality ITC data were obtained (Figure 5), with high signal-to-noise ratio over a range of temperatures, enabling accurate determination of association constants (K_A), enthalpy changes (ΔH), and the stoichiometry of binding (n) (Table 1). Consistent with the fluorescence titration, the ITC data fit well to a one-site model allowing the sites to be treated as identical and independent, simplifying further analysis.

ITC data were recorded at 5 deg intervals between 25 and 50 °C. Strong enthalpy/entropy compensation was observed, making the Gibbs free energy of binding (ΔG) nearly independent of temperature with a change of only 22 cal mol^{-1} K^{-1} over the temperature range (Figure 6). Tryptophan binding was found to be slightly temperature dependent as noted previously (*21*), with K_A values ranging from 9.75 × 10^6 M^{-1} at 25 °C to 1.17 × 10^6 M^{-1} at 50 °C.[1] The temperature dependence of the binding enthalpy was found to be linear in the measured temperature range, and a large negative change in heat capacity (ΔC_p) of −370 cal mol^{-1} K^{-1} was obtained from the temperature dependence of the binding enthalpy, $\partial\Delta H/\partial T$ (Figure 6). Analysis of the temperature dependence of the binding entropy, $T\partial\Delta S/\partial T$, yielded a value of 287.0 K for the characteristic temperature (T_s) at which the entropic contribution to binding (ΔS_{assoc}) is zero. Notably, the linearity of the ΔH versus T plot

[1] In these studies the temperature dependence of binding was found to be in the opposite direction from the previous studies. Although the origin of this discrepancy is unknown, it is small and may be a consequence of the differing conditions compared to the previous NMR-based experiment where the protein concentration (between 11 and 12 mM) was much higher than the K_d (~1 μM at 50 °C, Table 1).

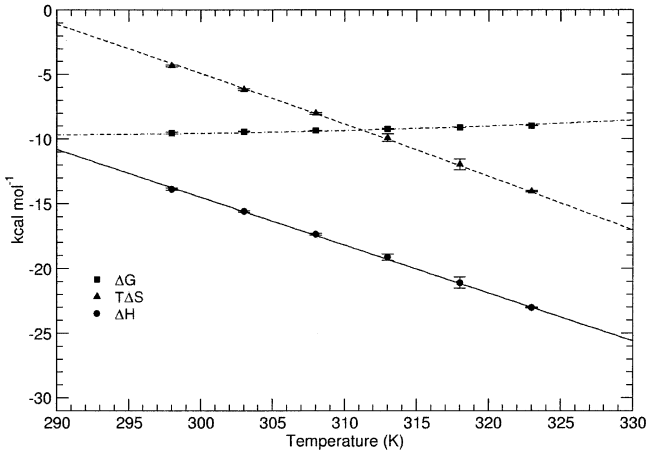

FIGURE 6: Temperature dependence of tryptophan binding to TRAP. The error bars represent the standard deviation in three repeat measurements at each temperature. Lines represent the best fit of the Gibbs−Helmholtz equation to the data. The data show the temperature dependence of the binding enthalpy (ΔH_{assoc}, circles), entropy ($T\Delta S_{assoc}$, triangles), and free energy change (ΔG_{assoc}, squares). A linear fit of the temperature dependence of the enthalpy yields a heat capacity change (ΔC_p) of −370 cal mol^{-1} K^{-1}, while fitting the temperature dependence of the free energy to the Gibbs−Helmholtz equation yields 287.0 K as the temperature (T_s) at which the association entropy change is zero.

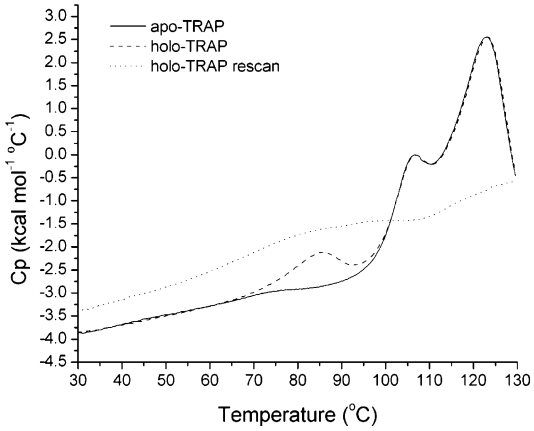

FIGURE 7: DSC of apo- and holo-TRAP. Scanning thermograms of apo- (solid line) and holo-TRAP (dashed line) reveal (1) the hyperthermal stability of the oligomeric protein, (2) the thermal separation between tryptophan dissociation and global unfolding of the protein, and (3) the linearity of the partial specific heat capacity in the temperature range studied by ITC (25−50 °C). Quantitative deconvolution analyses of these traces are not possible, however, due to the absence of a posttransition baseline and by lack of reversibility of the high-temperature global unfolding (as illustrated by the rescan of holo-TRAP, dotted line).

indicates that there is no measurable shift in a preexisting equilibrium between binding-competent and binding-incompetent conformational states of apo-TRAP, in the temperature range studied (*36*, *49*, *50*).

Thermal (DSC) scans of apo- and holo-TRAP (Figure 7) showed the partial specific heat capacity to be linear in the pretransition temperature range where ITC experiments were carried out. DSC analysis of apo- and holo-TRAP also showed the transition for ligand dissociation to be separate from that of global unfolding, occurring between 70 and 100 °C, with a midpoint temperature (T_m) of 85 °C. As a bimolecular association, the T_m for ligand dissociation would be expected to be concentration dependent; this was confirmed by a DSC scan at 5-fold lower concentration which

Table 2: Thermodynamics of the Binding-Coupled Folding of TRAP

Change in Solvent-Accessible Surface Area (ΔASA)	
absence of folding[a]	
polar	239 Å^2
nonpolar	378 Å^2
presence of folding[b]	
polar	1328 Å^2
nonpolar	1916 Å^2
Change in Heat Capacity (ΔC_p)	
expected from Trp burial[c]	−88 cal mol^{-1} K^{-1}
experimental	−370 cal mol^{-1} K^{-1}
upper limit for folding[d]	−427 cal mol^{-1} K^{-1}
Binding-Coupled Folding ($\mathscr{R}$)	
ITC	17−24 residues/monomer
NMR[e]	19 residues/monomer

[a] ΔASA for the burial of tryptophan was measured from the structure 1QAW (*14*); see Materials and Methods. [b] ΔASA for the burial of tryptophan and the 19 residues that exhibit ligand-dependent line broadening was measured from the structure 1QAW (*14*); see Materials and Methods. [c] Expected heat capacity change in the absence of folding was calculated from ΔASA (see footnote *a*) using eq 5. [d] Upper limit for the heat capacity change in the presence of folding if all of the residues go from an extended structure to a folded structure calculated from ΔASA (see footnote *b*) using eq 5. [e] Number of residues for which the NMR resonances are exchange-broadened beyond detection in apo-TRAP but are present in holo-TRAP and are located in the tryptophan- or RNA-binding sites.

showed the T_m to be slightly lower (83 °C) but still well separated from global unfolding. Assignment of the low-temperature transition to ligand dissociation was confirmed by monitoring the temperature-dependent dissociation of tryptophan by fluorescence (not shown). Interestingly, the observed independence of ligand dissociation and global unfolding in holo-TRAP is reminiscent of the thermal unfolding behavior of proteins with independent domains (*51*). Further, the high thermal stability for global unfolding of the oligomeric protein (>100 °C) is evident from the data. Nonreversibility of the high-temperature transition and absence of a posttransition baseline precluded detailed deconvolution analysis of the traces. The fact that there are two thermal transitions in addition to that associated with ligand binding merits more careful investigation but may indicate that thermal disassembly and denaturation of the oligomeric complex are not tightly coupled.

Solvent-Accessible Surface Area and the Expected ΔC_p. The heat capacity change upon protein folding or protein−ligand binding is often well described by solvation effects arising from changes in solvent-accessible surface area (ASA) (*23*−*30*). Coupling of conformational changes (*30*, *36*), including local protein folding (*28*, *52*), to ligand binding leads to a greater heat capacity change than that expected from surface burial (ΔASA) upon binding. The heat capacity change expected from the burial of polar and nonpolar surface area (ΔC_p^{calc}) has been parametrized (*29*, *53*−*55*) and can be calculated from the three-dimensional structure of the complex. The change in polar and nonpolar ASA due to burial of the tryptophan in the tryptophan-binding cavity was determined from the crystal structure of *B. stearothermophilus* TRAP in complex with tryptophan (1QAW) (*14*) using the program STC (*35*) (Table 2). From the change in ASA and the parameters of Spolar and Record (*28*), we calculated an expected change in heat capacity upon association (ΔC_p^{calc}) in the absence of protein folding of −88 cal M^{-1} K^{-1}; similar values are obtained with alternate parametrizations (*29*, *53*−*55*), including when aromatic and aliphatic carbons are treated differently (*29*). The difference between the calculated value and that measured by ITC (−370 cal M^{-1} K^{-1}) demonstrates that the large negative ΔC_p is poorly accounted for by surface burial, indicating a large contribution from other binding-coupled events.

Contributions to ΔC_p. Binding-associated changes in ΔC_p can have a number of origins (*23*, *30*, *36*): a change in solvent-accessible surface area (solvation effects), a change in the protonation state of either binding partner (proton linkage) (*37*), release of ions due to salt bridge formation during binding (ion linkage) (*38*), burial of structural water molecules (*56*, *57*), loss of translational and rotational degrees of freedom, changes in conformational entropy (*28*), and induced-fit conformational changes (*23*−*28*, *36*). To understand the nature of the binding event, all possible contributors to ΔC_p should be considered.

The intermolecular contacts between TRAP and bound tryptophan involve mainly hydrophobic contacts and polar interactions between groups that ionize outside of physiological pH ranges (*14*). This suggested that proton or ion linkage was unlikely to contribute to the heat capacity change; this expectation was confirmed by titrations of the binding partners in buffers with different enthalpies of ionization (*37*) and salt concentrations (*38*, *58*). The change in enthalpy (ΔH) of tryptophan binding to TRAP at 25 °C was measured in buffers with ionization enthalpies spanning 10 kcal mol^{-1} (Figure 8). The enthalpy of tryptophan binding was found to be nearly independent of the heat of ionization of the buffer. The binding affinity of TRAP for tryptophan was similarly found to be largely independent of salt concentration (Figure 8). Therefore, the contributions to the observed ΔC_p from proton and ion linkage are very small.

Burial of structural water molecules in molecular interfaces has been implicated in contributing to the measured ΔC_p (*56*, *57*), so possible contribution from bound water molecules was considered. Examination of the tryptophan-binding sites in *B. stearothermophilus* holo-TRAP alone (1QAW; 2.5 Å resolution) (*14*) and bound to RNA (1C9S; 1.9 Å solution) (*13*) reveals a surface-exposed water molecule bound between the carboxylate group of the tryptophan ligand and the side chain of His49 in the majority of the binding pockets. Estimates for the contribution of burying a water molecule in an interface (i.e., transfer of a water molecule from solution to the protein) have been obtained from sorption isotherms (*59*), the standard enthalpies of anhydrous and hydrated inorganic salts (*60*), and from high-resolution structural data (*57*). These analyses suggest an upper limit of −12 cal mol^{-1} K^{-1} for the contribution to ΔC_p of burying a water molecule in an interface. Use of these estimates suggests that the contribution to the observed ΔC_p of crystallographically observed water molecules in the binding cavity is small compared to the observed ΔC_p (−370 cal K^{-1} mol^{-1}). It should be noted, however, that the nature of these bound water-mediated contributions to ΔC_p are not yet well understood, and it has been proposed they can be insignificant (*60*) or even significantly larger (*56*, *61*, *62*).

Binding-Coupled Folding of TRAP. Changes in structure and conformational mobility that accompany ligand binding strongly impact measured heat capacity changes (*23*, *28*, *30*). We followed the approach of Spolar and Record (*28*), which provides an empirical estimate of the number of residues involved in coupled folding ($\mathscr{R}$) from the experimentally

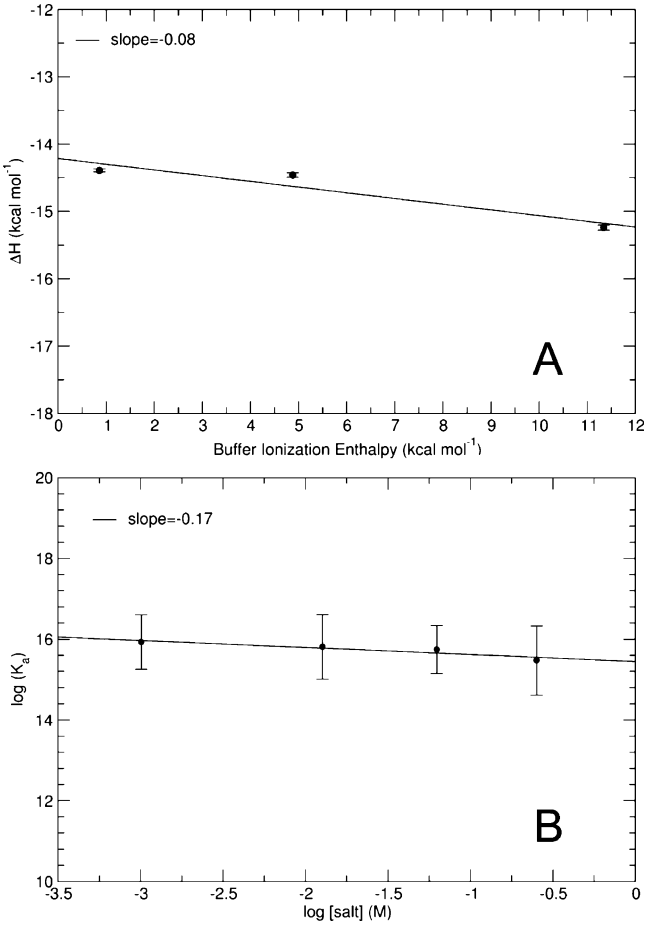

FIGURE 8: Proton and ion linkage. (A) There is very little change in the binding enthalpy in titrations of tryptophan into TRAP in the presence of buffers with different enthalpies of ionization [a slope of −0.08 compared to a slope of ∼1 in the case of a single proton uptake (*37*, *71*)], demonstrating that changes in protonation state upon binding do not contribute significantly to the observed heat capacity change. (B) Changes in salt concentration show little effect on the association constant (a slope of −0.17), demonstrating that uptake or release of ions also does not contribute significantly to the observed heat capacity change (*38*, *58*).

measured ΔC_p (eq 7 in Materials and Methods). Using this approach, neglecting contributions from trapped interfacial water, and using a value for the per-residue entropic loss ($\Delta S_{\mathscr{R}}$) of −5.6 cal K^{-1} (mol of residue)$^{-1}$ (*28*), we find that the excess heat capacity change corresponds to the folding of 18 residues per monomer upon tryptophan binding to TRAP (eq 7 in Materials and Methods and Table 2). If we assume that the crystallographically observed water molecules contribute up to −12 cal mol^{-1} K^{-1} (*57*, *59*, *60*) to the measured heat capacity, this lowers the estimate of $\mathscr{R}$ to 17 residues per monomer. Use of −4.1 cal K^{-1} (mol of residue)$^{-1}$ for $\Delta S_{\mathscr{R}}$ (*40*) increases the estimate to 23 and 24 residues with and without a contribution from water burial, respectively. (We note, however, that there remains considerable disagreement in the literature over the magnitude of the contribution of ΔS_{rt} to the overall entropy of association and has been proposed to be much smaller, on the order of 5 ± 4 cal mol^{-1} K^{-1} (*63*); use of this smaller value would increase $\mathscr{R}$ by ∼9 residues.) Thus, following this empirical approach we find that the measured ΔC_p corresponds to ligand-coupled loss of conformational mobility (i.e., folding) of 17−24 residues ($\mathscr{R}$) per monomer of TRAP (Table 2); these numbers correspond to roughly one-fourth to one-third of the 74 residues in each protomer.

The results of these calorimetric estimations (17−24 residues folded) are in reasonable agreement with NMR studies which showed that 19 residues in the tryptophan- and RNA-binding regions of TRAP were observed in the presence of tryptophan but were severely exchange-broadened in the absence (*21*) (shown in green in Figures 1 and 2). As a check on the underlying approximations, we tested whether folding of these 19 residues would generate a ΔC_p comparable to that measured experimentally. We computed the ΔASA for binding-coupled folding of the 19 residues (see Materials and Methods) and obtained a ΔC_p of −427 cal mol^{-1} K^{-1} for a transition between the fully extended and exposed conformation and the fully folded conformation (Table 2). Because the unfolded residues are in loops between regions that remain structured even in apo-TRAP, this number would be expected to overestimate the possible ASA change but is of similar magnitude to the experimentally measured value of −370 cal mol^{-1} K^{-1}.

The agreement between these quantitative and qualitative analyses leads us to conclude that most of the ΔC_p measured by ITC arises from the same ligand-coupled changes in protein structure and dynamics (i.e., folding) that lead to the observed differences in the spectra between the apo/inactivated and holo/activated states of TRAP. Those structural and dynamic changes are localized principally to the RNA- and tryptophan-binding regions of TRAP (Figure 2). On the other hand, it is clear from the effect of ligand binding on the H/D exchange rates (Figures 2 and 4) that the thermodynamic consequences of ligand binding are not entirely limited to those 19 residues and affect the structure, dynamics, and thermodynamics of (at least those) additional residues.

Binding-Coupled Folding and a Model for Allosteric Control of TRAP. The data presented lend support for a model for allosteric control of TRAP in which tryptophan-dependent coupled folding of the tryptophan- and RNA-binding residues control RNA binding (Figure 1) (*21*). In this model, residues in the tryptophan- and RNA-binding region of TRAP are dynamically disordered in the apoprotein [i.e., a preexisting conformational equilibrium (*48*)], preventing RNA binding and allowing entry of the tryptophan to its binding site. Initial tryptophan binding to one state of the protein induces ordering of the tryptophan- and RNA-binding residues, thereby shifting the equilibrium, forming a stable RNA-binding interface, and activating TRAP to bind to its RNA target. We propose that the loss of conformational mobility (*28*) [reduction in "soft vibrational modes"(*23*)] in this tryptophan- and RNA-binding region upon ligand binding is responsible for much of the large negative heat capacity detected in the calorimetric experiments.

However, it is worth noting that because the tryptophan ligand is completely buried in holo-TRAP (*14*), the binding-competent conformation of apo-TRAP must be distinct from that of holo-TRAP. Consequently, it seems necessary that, upon tryptophan binding, TRAP must also undergo an induced-fit conformational change (*64*) from a binding-competent state to the ligand-buried holo state. Indeed, the absence of a significant population of a holo-like state in apo-TRAP is essential from a regulatory standpoint: because RNA binds very tightly to the activated form of TRAP, if that state were significantly populated in the absence of

ligand, RNA binding would drive the equilibrium toward the activated form, thereby degrading the effectiveness of regulation. The equilibrium thermodynamic parameters measured in this study capture, without distinction, both the initial binding event and the ensuing conformational change.

Since the tryptophan is completely buried in tryptophan-activated TRAP, it seems reasonable that some of the residues in the tryptophan-binding site must remain dynamic even in the RNA-bound state in order to allow TRAP to remain sensitive to the levels of intracellular tryptophan. This prediction is in agreement with the observation that some NMR resonances from the tryptophan-binding region remain exchange-broadened in tryptophan-activated TRAP (regions in red in Figures 1 and 2) (*21*). This observation is also consistent with the observed lack of cooperativity in tryptophan binding (Figures 3 and 5), as persistent dynamics would result in, at best, weak coupling between adjacent binding sites. If, on the contrary, ligand binding were to lead to complete rigidification of one interprotomer interface, conventional allostery models (*43*, *65*−*68*) would predict strong coupling and lead to undesirably high affinity tryptophan binding and loss of regulation.

The apparent independence of thermally induced ligand dissociation and protein denaturation (Figure 7) merits a final point of discussion. Tight coupling between ligand binding and global unfolding of proteins has been widely observed, and deconvolution of thermograms from such systems has been used to obtain the relevant thermodynamic parameters (*69*, *70*). In contrast, the observed independence of local and global unfolding in holo-TRAP is reminiscent of the thermal unfolding behavior of proteins with independent domains (*51*). The fascinating and complex mystery of how TRAP regulates transcription is hereby further accentuated by the observation that TRAP activation seems to involve the discrete stabilization of an RNA-binding "domain" that is thermodynamically distinct from the underlying oligomeric protein scaffold that supports it.

ACKNOWLEDGMENT

The authors thank J. Cowan (OSU) for access to instrumentation, V. Fresca (Microcal), J. Cowan, S. Walsh (OSU), and members of the Foster laboratory for helpful discussions, and S. Edmondson (UAH) and J. Ladbury (UCL) for critical reading of the manuscript.

SUPPORTING INFORMATION AVAILABLE

Replicate thermograms of tryptophan-TRAP titrations over the temperature range of 25−55 °C. This material is available free of charge via the Internet at http://pubs.acs.org.

REFERENCES

1. Babitzke, P., and Yanofsky, C. (1993) Reconstitution of *Bacillus subtilis* trp attenuation in vitro with TRAP, the trp RNA-binding attenuation protein, *Proc. Natl. Acad. Sci. U.S.A. 90*, 133−137.
2. Gollnick, P. (1994) Regulation of the *Bacillus subtilis* trp operon by an RNA-binding protein, *Mol. Microbiol. 11*, 991−997.
3. Gollnick, P., and Babitzke, P. (2002) Transcription attenuation, *Biochim. Biophys. Acta 1577*, 240−250.
4. Babitzke, P. (1997) Regulation of tryptophan biosynthesis: Trping the TRAP or how *Bacillus subtilis* reinvented the wheel, *Mol. Microbiol. 26*, 1−9.
5. Babitzke, P. (2004) Regulation of transcription attenuation and translation initiation by allosteric control of an RNA-binding protein: the *Bacillus subtilis* TRAP protein, *Curr. Opin. Microbiol. 7*, 132−139.
6. Du, H., and Babitzke, P. (1998) trp RNA-binding attenuation protein-mediated long distance RNA refolding regulates translation of trpE in *Bacillus subtilis*, *J. Biol. Chem. 273*, 20494−20503.
7. Merino, E., Babitzke, P., and Yanofsky, C. (1995) trp RNA-binding attenuation protein (TRAP)-trp leader RNA interactions mediate translational as well as transcriptional regulation of the *Bacillus subtilis* trp operon, *J. Bacteriol. 177*, 6362−6370.
8. Sarsero, J. P., Merino, E., and Yanofsky, C. (2000) A *Bacillus subtilis* gene of previously unknown function, yhaG, is translationally regulated by tryptophan-activated TRAP and appears to be involved in tryptophan transport, *J. Bacteriol. 182*, 2329−2331.
9. Yakhnin, H., Babiarz, J. E., Yakhnin, A. V., and Babitzke, P. (2001) Expression of the *Bacillus subtilis* trpEDCFBA operon is influenced by translational coupling and Rho termination factor, *J. Bacteriol. 183*, 5918−5926.
10. Yakhnin, H., Zhang, H., Yakhnin, A. V., and Babitzke, P. (2004) The trp RNA-binding attenuation protein of *Bacillus subtilis* regulates translation of the tryptophan transport gene trpP (yhaG) by blocking ribosome binding, *J. Bacteriol. 186*, 278−286.
11. Yang, M., de Saizieu, A., van Loon, A. P., and Gollnick, P. (1995) Translation of trpG in *Bacillus subtilis* is regulated by the trp RNA-binding attenuation protein (TRAP), *J. Bacteriol. 177*, 4272−4278.
12. Antson, A. A., Otridge, J., Brzozowski, A. M., Dodson, E. J., Dodson, G. G., Wilson, K. S., Smith, T. M., Yang, M., Kurecki, T., and Gollnick, P. (1995) The structure of trp RNA-binding attenuation protein, *Nature 374*, 693−700.
13. Antson, A. A., Dodson, E. J., Dodson, G., Greaves, R. B., Chen, X., and Gollnick, P. (1999) Structure of the trp RNA-binding attenuation protein, TRAP, bound to RNA, *Nature 401*, 235−242.
14. Chen, X., Antson, A. A., Yang, M., Li, P., Baumann, C., Dodson, E. J., Dodson, G. G., and Gollnick, P. (1999) Regulatory features of the trp operon and the crystal structure of the trp RNA-binding attenuation protein from *Bacillus stearothermophilus*, *J. Mol. Biol. 289*, 1003−1016.
15. Babitzke, P., and Yanofsky, C. (1995) Structural features of L-tryptophan required for activation of TRAP, the trp RNA-binding attenuation protein of *Bacillus subtilis*, *J. Biol. Chem. 270*, 12452−12456.
16. Yang, M., Chen, X., Militello, K., Hoffman, R., Fernandez, B., Baumann, C., and Gollnick, P. (1997) Alanine-scanning mutagenesis of *Bacillus subtilis* trp RNA-binding attenuation protein (TRAP) reveals residues involved in tryptophan binding and RNA binding, *J. Mol. Biol. 270*, 696−710.
17. Elliott, M. B., Gottlieb, P. A., and Gollnick, P. (1999) Probing the TRAP-RNA interaction with nucleoside analogs, *RNA 5*, 1277−1289.
18. Elliott, M., Gottlieb, P., and Gollnick, P. (2001) Using nucleotide analogs to probe protein-RNA interactions, *Methods 23*, 255−263.
19. Elliott, M. B., Gottlieb, P. A., and Gollnick, P. (2001) The mechanism of RNA binding to TRAP: initiation and cooperative interactions, *RNA 7*, 85−93.
20. Li, P. T., Scott, D., and Gollnick, P. (2002) Creating hetero-11-mers composed of wild-type and mutant subunits to study RNA binding to TRAP, *J. Biol. Chem. 227*, 11838−11844.
21. McElroy, C., Manfredo, A., Wendt, A., Gollnick, P., and Foster, M. (2002) TROSY-NMR studies of the 91kDa TRAP protein reveal allosteric control of a gene regulatory protein by ligand-altered flexibility, *J. Mol. Biol. 323*, 463−473.
22. Snyder, D., Lary, J., Chen, Y., Gollnick, P., and Cole, J. L. (2004) Interaction of the trp RNA-binding attenuation protein (TRAP) with anti-TRAP, *J. Mol. Biol. 338*, 669−682.
23. Sturtevant, J. M. (1977) Heat capacity and entropy changes in processes involving proteins, *Proc. Natl. Acad. Sci. U.S.A. 74*, 2236−2240.
24. Baldwin, R. L. (1986) Temperature dependence of the hydrophobic interaction in protein folding, *Proc. Natl. Acad. Sci. U.S.A. 83*, 8069−8072.
25. Privalov, P. L., and Gill, S. J. (1988) Stability of protein structure and hydrophobic interaction, *Adv. Protein Chem. 39*, 191−234.
26. Privalov, P. L., and Khechinashvili, N. N. (1974) A thermodynamic approach to the problem of stabilization of globular protein structure: a calorimetric study, *J. Mol. Biol. 86*, 665−684.
27. Spolar, R. S., Ha, J. H., and Record, M. T., Jr. (1989) Hydrophobic effect in protein folding and other noncovalent processes involving proteins, *Proc. Natl. Acad. Sci. U.S.A. 86*, 8382−8385.

28. Spolar, R. S., and Record, M. T., Jr. (1994) Coupling of local folding to site-specific binding of proteins to DNA, *Science 263*, 777−784.
29. Makhatadze, G. I., and Privalov, P. L. (1995) Energetics of protein structure, *Adv. Protein Chem. 47*, 307−425.
30. Prabhu, N. V., and Sharp, K. A. (2005) Heat capacity in proteins, *Annu. Rev. Phys. Chem. 56*, 521−548.
31. Glasoe, P. K., and Long, F. A. (1960) Use of glass electrodes to measure acidities in deuterium oxide, *J. Phys. Chem. 64*, 188−190.
32. Pervushin, K., Riek, R., Wider, G., and Wuthrich, K. (1997) Attenuated T2 relaxation by mutual cancellation of dipole-dipole coupling and chemical shift anisotropy indicates an avenue to NMR structures of very large biological macromolecules in solution, *Proc. Natl. Acad. Sci. U.S.A. 94*, 12366−12371.
33. Gill, S. C., and von Hippel, P. H. (1989) Calculation of protein extinction coefficients from amino acid sequence data, *Anal. Biochem. 182*, 319−326.
34. Fasman, G. D. (1975) *Handbook of Biochemistry and Molecular Biology*, 3d ed., CRC Press, Cleveland, OH.
35. Lavigne, P., Bagu, J. R., Boyko, R., Willard, L., Holmes, C. F., and Sykes, B. D. (2000) Structure-based thermodynamic analysis of the dissociation of protein phosphatase-1 catalytic subunit and microcystin-LR docked complexes, *Protein Sci. 9*, 252−264.
36. Eftink, M. R., Anusiem, A. C., and Biltonen, R. L. (1983) Enthalpy-entropy compensation and heat capacity changes for protein-ligand interactions: general thermodynamic models and data for the binding of nucleotides to ribonuclease A, *Biochemistry 22*, 3884−3896.
37. Baker, B. M., and Murphy, K. P. (1996) Evaluation of linked protonation effects in protein binding reactions using isothermal titration calorimetry, *Biophys. J. 71*, 2049−2055.
38. Lohman, T. M., Overman, L. B., Ferrari, M. E., and Kozlov, A. G. (1996) A highly salt-dependent enthalpy change for *Escherichia coli* SSB protein-nucleic acid binding due to ion-protein interactions, *Biochemistry 35*, 5272−5279.
39. Murphy, K. P., Privalov, P. L., and Gill, S. J. (1990) Common features of protein unfolding and dissolution of hydrophobic compounds, *Science 247*, 559−561.
40. Robertson, A. D., and Murphy, K. P. (1997) Protein structure and the energetics of protein stability, *Chem. Rev. 97*, 1251−1268.
41. Koradi, R., Billeter, M., and Wuthrich, K. (1996) MOLMOL: a program for display and analysis of macromolecular structures, *J. Mol. Graphics 14*, 51−55, 29−32.
42. Creed, D. (1984) The photophysics and photochemistry of the near-UV absorbing amino acids. I. Tryptophan and its simple derivatives, *Photochem. Photobiol. 39*, 537−562.
43. Saroff, H. A., and Kiefer, J. E. (1997) Analysis of the binding of ligands to large numbers of sites: the binding of tryptophan to the 11 sites of the trp RNA-binding attenuation protein, *Anal. Biochem. 247*, 138−142.
44. Deleage, G., and Geourjon, C. (1993) An interactive graphic program for calculating the secondary structure content of proteins from circular dichroism spectrum, *Comput. Appl. Biosci. 9*, 197−199.
45. Sreerama, N., Venyaminov, S. Y., and Woody, R. W. (2000) Estimation of protein secondary structure from circular dichroism spectra: inclusion of denatured proteins with native proteins in the analysis, *Anal. Biochem. 287*, 243−251.
46. Freskgard, P. O., Martensson, L. G., Jonasson, P., Jonsson, B. H., and Carlsson, U. (1994) Assignment of the contribution of the tryptophan residues to the circular dichroism spectrum of human carbonic anhydrase II, *Biochemistry 33*, 14281−14288.
47. Grishina, I. B., and Woody, R. W. (1994) Contributions of tryptophan side chains to the circular dichroism of globular proteins: exciton couplets and coupled oscillators, *Faraday Discuss.*, 245−262.
48. Tsai, C. J., Kumar, S., Ma, B., and Nussinov, R. (1999) Folding funnels, binding funnels, and protein function, *Protein Sci. 8*, 1181−1190.
49. Bruzzese, F. J., and Connelly, P. R. (1997) Allosteric properties of inosine monophosphate dehydrogenase revealed through the thermodynamics of binding of inosine 5′-monophosphate and mycophenolic acid. Temperature dependent heat capacity of binding as a signature of ligand-coupled conformational equilibria, *Biochemistry 36*, 10428−10438.
50. Privalov, P. L., Jelesarov, I., Read, C. M., Dragan, A. I., and Crane-Robinson, C. (1999) The energetics of HMG box interactions with DNA: thermodynamics of the DNA binding of the HMG box from mouse sox-5, *J. Mol. Biol. 294*, 997−1013.
51. Privalov, P. L. (1982) Stability of proteins. Proteins which do not present a single cooperative system. *Adv. Protein Chem. 35*, 1−104.
52. Ha, J. H., Spolar, R. S., and Record, M. T., Jr. (1989) Role of the hydrophobic effect in stability of site-specific protein-DNA complexes, *J. Mol. Biol. 209*, 801−816.
53. Spolar, R. S., Livingstone, J. R., and Record, M. T., Jr. (1992) Use of liquid hydrocarbon and amide transfer data to estimate contributions to thermodynamic functions of protein folding from the removal of nonpolar and polar surface from water, *Biochemistry 31*, 3947−3955.
54. Murphy, K. P., and Freire, E. (1992) Thermodynamics of structural stability and cooperative folding behavior in proteins, *Adv. Protein Chem. 43*, 313−361.
55. Myers, J. K., Pace, C. N., and Scholtz, J. M. (1995) Denaturant *m* values and heat capacity changes: relation to changes in accessible surface areas of protein unfolding, *Protein Sci. 4*, 2138−2148.
56. Bergqvist, S., Williams, M. A., O'Brien, R., and Ladbury, J. E. (2004) Heat capacity effects of water molecules and ions at a protein-DNA interface, *J. Mol. Biol. 336*, 829−842.
57. Morton, C. J., and Ladbury, J. E. (1996) Water-mediated protein-DNA interactions: the relationship of thermodynamics to structural detail, *Protein Sci. 5*, 2115−2118.
58. Holbrook, J. A., Tsodikov, O. V., Saecker, R. M., and Record, M. T., Jr. (2001) Specific and non-specific interactions of integration host factor with DNA: thermodynamic evidence for disruption of multiple IHF surface salt-bridges coupled to DNA binding, *J. Mol. Biol. 310*, 379−401.
59. Bryan, W. P. (1980) The thermodynamics of water−protein interactions, *J. Theor. Biol. 87*, 639−661.
60. Dunitz, J. (1994) The entropic cost of bound water in crystals and biomolecules, *Science 264*, 670.
61. Holdgate, G. A., Tunnicliffe, A., Ward, W. H., Weston, S. A., Rosenbrock, G., Barth, P. T., Taylor, I. W., Pauptit, R. A., and Timms, D. (1997) The entropic penalty of ordered water accounts for weaker binding of the antibiotic novobiocin to a resistant mutant of DNA gyrase: a thermodynamic and crystallographic study, *Biochemistry 36*, 9663−9673.
62. Cooper, A. (2005) Heat capacity effects in protein folding and ligand binding: a re-evaluation of the role of water in biomolecular thermodynamics, *Biophys. Chem. 115*, 89−97.
63. Tamura, A., and Privalov, P. L. (1997) The entropy cost of protein association, *J. Mol. Biol. 273*, 1048−1060.
64. Koshland, J. D. E. (1958) Application of a theory of enzyme specificity to protein synthesis, *Proc. Natl. Acad. Sci. U.S.A. 44*, 98−104.
65. Changeux, J. P., Gerhart, J. C., and Schachman, H. K. (1968) Allosteric interactions in aspartate transcarbamylase. I. Binding of specific ligands to the native enzyme and its isolated subunits, *Biochemistry 7*, 531−538.
66. Cooper, A., and Dryden, D. T. (1984) Allostery without conformational change. A plausible model, *Eur. Biophys. J. 11*, 103−109.
67. Jardetzky, O. (1996) Protein dynamics and conformational transitions in allosteric proteins, *Prog. Biophys. Mol. Biol. 65*, 171−219.
68. Perutz, M. F. (1989) Mechanisms of cooperativity and allosteric regulation in proteins, *Q. Rev. Biophys. 22*, 139−237.
69. Brandts, J. F., and Lin, L. N. (1990) Study of strong to ultratight protein interactions using differential scanning calorimetry, *Biochemistry 29*, 6927−6940.
70. Jelesarov, I., and Bosshard, H. R. (1999) Isothermal titration calorimetry and differential scanning calorimetry as complementary tools to investigate the energetics of biomolecular recognition, *J. Mol. Recognit. 12*, 3−18.
71. Jelesarov, I., and Bosshard, H. R. (1994) Thermodynamics of ferredoxin binding to ferredoxin:$NADP^+$ reductase and the role of water at the complex interface, *Biochemistry 33*, 13321−13328.
72. Frauenfelder, H., Parak, F., and Young, R. D. (1988) Conformational substates in proteins, *Annu. Rev. Biophys. Chem. 17*, 451−479.

BI0526074